

Cite this article as: Chen Dongdong, Qin Junhu, Gan Youwei, et al. Effect of Ag Content on Formation and Growth of Intermetallic Compounds in Sn-20Bi-0.7Cu Solder[J]. Rare Metal Materials and Engineering, 2023, 52(02): 502-507.

ARTICLE

Effect of Ag Content on Formation and Growth of Intermetallic Compounds in Sn-20Bi-0.7Cu Solder

Chen Dongdong¹, Qin Junhu², Gan Youwei¹, Zhang Xin², Bai Hailong³, Zhao Lingyan³, Yi Jianhong¹, Yan Jikang^{1,4}

¹ Faculty of Materials Science and Engineering, Kunming University of Science and Technology, Kunming 650093, China; ² Tin Products Manufacturing Co., Ltd of YTCL, Kunming 650217, China; ³ R&D Center, Yunnan Tin Group (Holding) Co., Ltd, Kunming 650000, China; ⁴ School of Engineering, Southwest Petroleum University, Nanchong 637001, China

Abstract: The interfacial reactions and growth kinetics of Sn-20Bi-0.7Cu-xAg ($x=0.1, 0.4, 0.7, 1.0, 1.5$, wt%) were investigated during solid-state aging. The effects of chemical composition on the structure and the growth of interface under high temperature and high humidity conditions were studied experimentally and numerically. In order to determine the long-term reliability of the solder joints, thermal accelerated aging tests were performed for 0, 10, 30, 50, 100, 200 and 500 h under 85 °C and 85% relative humidity conditions. The surface morphology, thickness, and distribution of interface compounds were observed by scanning electron microscope. The nucleation surface and growth direction of β -Sn were clarified. The phases were determined at the interface and the alloy matrix. Results show that with increasing the Ag content, the growth of the Cu_6Sn_5 layer is suppressed. The growth kinetics of intermetallic compound ($\text{Cu}_6\text{Sn}_5+\text{Cu}_3\text{Sn}$) remains a diffusion-controlled process during the isothermal aging. The scallop-type Cu_6Sn_5 phase disappears at later aging stages, suggesting that the growth mechanism changes to the steady growth in the direction perpendicular to the interface. Besides, the results reveal that Ag_3Sn effectively slows down the growth kinetics of Cu_6Sn_5 .

Key words: Sn-20Bi-0.7Cu; intermetallic compounds; solidification; interface structure; growth kinetics

Toxic Pb in Sn-Pb solder has swarmed into the waste streams of electronic industries in the past years, and restrictive regulations have been proposed to make extensive usage of a variety of lead-free solders possible^[1-3]. Sn-Bi solder has been considered as one of the most promising lead-free products as a substitute for conventional Sn-Pb solders. Its low melting point makes it widely used in some individual situations for soldering^[4-5]. Many researchers have studied low Cu lead-free solders. For example, Miao^[6] studied binary eutectic Sn-Bi and ternary Sn-Bi-1wt% Cu for solder joints, and found that the addition of 1wt% Cu has little effect on the contact angle of the eutectic Sn-Bi solder alloy with various metallization layers. Some cracks are generated, however, through the Al_2O_3 substrate. The contact resistance of the solder/Cu joint does not increase after thermal cycling since

the resistivity of Cu_6Sn_5 is lower than that of the solder. The coarsening rate of the Bi-rich phase in the solder joint under thermal aging at 120 °C is reduced by adding 1wt% Cu to the Sn-58Bi solder^[7-8]. At present, most investigations still focus on the effects of alloy element addition on properties for ternary and multi-element alloys. Still, studies ignore the growth kinetics of the alloy interface in the Sn-Bi-Cu/Cu layer.

Butrymowicz^[9] reviewed diffusion of Sn-Cu alloys in 1977. In Cu solid solutions, Sn is the fast diffuser^[10-11]. In addition, Cu is known to be an extremely fast interstitial diffuser in the c -direction in Sn. However, in the present research, we focused on diffusion in the intermetallic compounds. This subject has been studied using diffusion couples proposed by Hopkins et al^[12]. The dissolved metal and a layer of

Received date: August 08, 2022

Foundation item: Major Science and Technology Project in Yunnan Province-New Material Special Project (202105AE160028); Yunnan Province Transformation Research Institute Technology Development Research Project-Innovation Guidance and Technology Enterprise Cultivation Plan (202202AB080001); Fundamental Research and Applied Basic Research Enterprise Joint Project Between Yunnan Provincial Department of Science and Technology and Yunnan Tin Group (Holding) Company Limited (202101BC070001-010)

Corresponding author: Yan Jikang, Ph. D., Professor, School of Engineering, Southwest Petroleum University, Nanchong 637001, P. R. China, E-mail: yanjk@swpu.edu.cn

Copyright © 2023, Northwest Institute for Nonferrous Metal Research. Published by Science Press. All rights reserved.

intermetallic compound (IMC) form at the metal-solder interface. Due to thermally activated solid-state diffusion mechanisms, the intermetallic layer continues to grow after solidification. The formation and growth of intermetallic affect the solderability and reliability of electronic solder joints at the solder/substrate interface^[13]. Due to the high concentration of Sn, eutectic Sn-Bi-Cu solders form Cu-Sn intermetallic compounds on the copper substrate^[14]. However, Sn-Bi-Cu solders possess a generally lower melting temperature and higher Sn content compared to lead-containing solders. Thus, the formation and growth of the IMC layer are tardier in Sn-Bi-Cu solder joint, resulting in brittle fractures and improving the thermal fatigue life of the joint. But researchers seem to ignore its interface issues.

In this study, the microstructure and interface layers of Sn-20Bi-0.7Cu-*x*Ag/Cu (*x*=0.1, 0.4, 0.7, 1.0, 1.5, wt%) were studied. The solder joints were controlled under the condition of high temperature and high humidity. The surface morphology, thickness, and distribution of compounds were observed by scanning electron microscope (SEM) and transmission electron microscope (TEM). Finally, the relevant thermodynamic and growth kinetic parameters were calculated. The present results demonstrate affecting mechanism of Ag content on interface layer growth. It can widen the application of Sn-20Bi-0.7Cu-*x*Ag lead-free solders.

1 Experiment

A certain amount of Sn spheres were weighed and heated in an intermediate frequency furnace. When the Sn sphere was completely melted, Bi, Sn-3Ag and Sn-10Cu (wt%) were added and stirred, and then kept at 240 °C for 2 h. The solder alloy solution was cast into an ingot at 25 °C. Solder joints were prepared using a MUST SYSTEM III instrument. First, the solder alloy liquid was heated to 240 °C. Second, the solder was welded to a copper plate. Finally, the solder joints were immersed in hydrochloric acid to remove the oxide film on the surface. The tests were carried out in a constant temperature and humidity box (ec-85mhhp-c) at 85 °C and 85% relative humidity (RH). Solder joint preparation and aging process are shown in Fig.1.

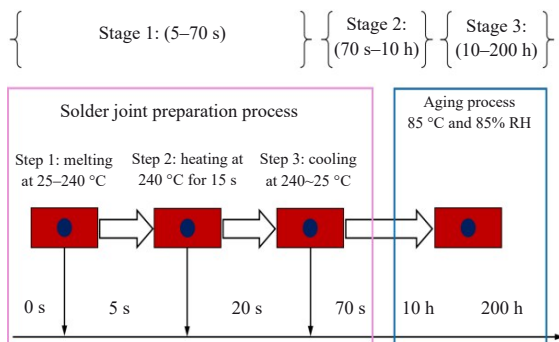


Fig.1 Solder joints preparation and aging process

2 Results

2.1 Solidification simulation

The cooling solidification curves and phase composition diagrams are calculated by Thermo-Calc (2020a), as shown in Fig.2. Since the database of quaternary alloys is not perfect, we choose two ternary alloys separately for thermodynamic analysis. Fig.2a and 2b demonstrate that the melting point of Sn-1.0Ag-0.7Cu is higher than that of Sn-20Bi-0.7Cu.

With the addition of Bi, the alloy solidifies and precipitates Sn-58Bi eutectics, which effectively reduce the melting point of the solder alloy, but the liquidus temperature is stable. At this time, the melting range increases, which will reduce the wettability of the solder alloy. The calculation result is consistent with the experimental result of Zhang^[15]. When the temperature is 187 °C, η' -Cu₆Sn₅ is transformed into η -Cu₆Sn₅ in Fig.2c and 2d^[16]. According to the binary phase diagram of Cu-Sn, there are two main crystal structure types of Cu₆Sn₅. When the temperature is below 186 °C, the stable configuration is η' -Cu₆Sn₅, which belongs to the monoclinic crystal system. When the temperature exceeds 186 °C, Cu₆Sn₅ is transformed into η -Cu₆Sn₅ with a hexagonal structure. The main phase is β -Sn. The content of Cu₆Sn₅ IMC is the least, not exceeding 2.5wt%.

Fig.3 shows the XRD patterns of the Sn-20Bi-0.7Cu-*x*Ag (*x*=0.1, 0.4, 0.7, 1.0, 1.5) alloys. The peaks at 79.3°, 44.8°, 39.6°, 37.8° and 27.12° are indexed to Cu₆Sn₅, β -Sn, Ag₃Sn, Cu₃Sn, and Bi, respectively. Notably, the characteristic peaks of Cu₆Sn₅ are weaker than those of Sn, which shows that the sample has excessive Sn in the Cu₆Sn₅. The diffraction peaks of both β -Sn and Bi are sharp and intense, indicating their high crystalline nature. No impurity peaks are observed, confirming the high purity of the samples. However, although the content of Ag increases to 1.5wt%, it is nearly the same as the case with 0.1wt% Ag. It can be seen that the phase composition of the sample is steady. We further confirm that the phase compositions of solders Sn-20Bi-0.7Cu-*x*Ag are β -Sn, Cu₆Sn₅, Ag₃Sn, and SnBi eutectic. The experimental results are in excellent agreement with the calculated results.

2.2 Interface compound layer structure

During reflow soldering, the solder melts, dissolves, and diffuses into the substrate. The gradient of the chemical potential between different materials leads to the interdiffusion of different atoms at the solder/substrate boundary. A local equilibrium allows IMCs (Cu₆Sn₅+Cu₃Sn) to form at the solder/Cu substrate interface. At the solder/Cu substrate interface, Cu₆Sn₅ phase will be first generated, which will react with Cu to form Cu₃Sn as the aging proceeds^[17]. The Cu₆Sn₅ growth is governed by the reaction between Cu and Sn atoms present in the Cu₆Sn₅/solder interface, as stated by Eq. (3). According to Eq. (2), Cu atoms diffused from the metal substrate to the Cu₆Sn₅/solder interface are significantly reduced as the Cu₃Sn layer thickness increases with prolonging aging time. At the same time, the supply of Cu from the solder is limited, since most of the Cu atoms have been used to form Cu₆Sn₅ particles in the solder matrix.

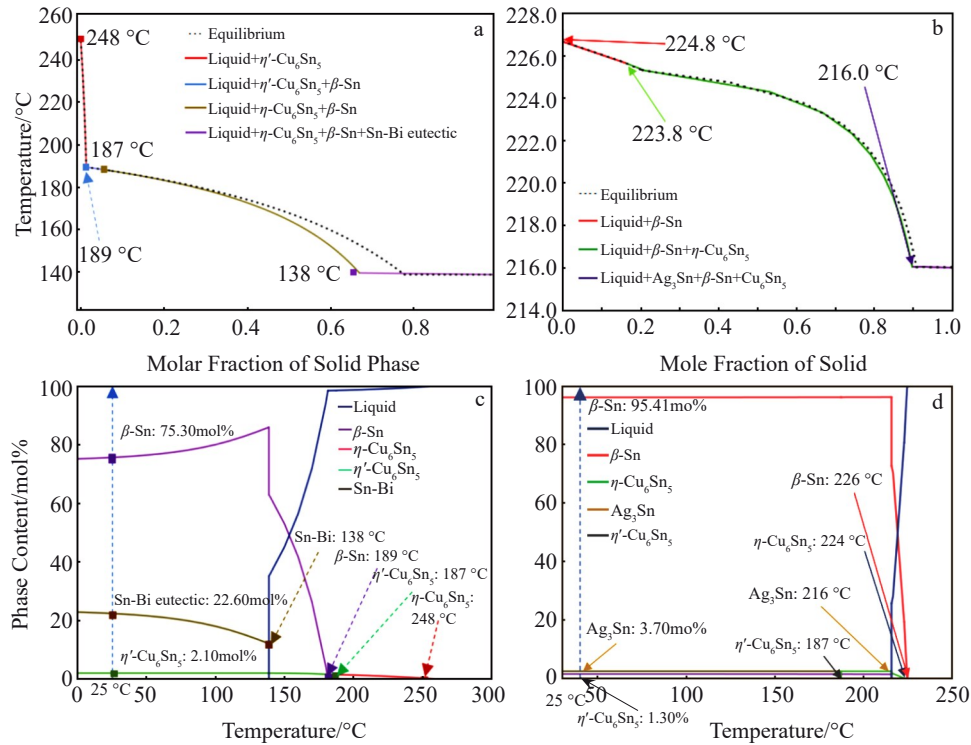


Fig.2 Cooling solidification curves (a, b) and phase composition diagrams (c, d)^[16] for Sn-20Bi-0.7Cu (a, c) and Sn-1.0Ag-0.7Cu (b, d)

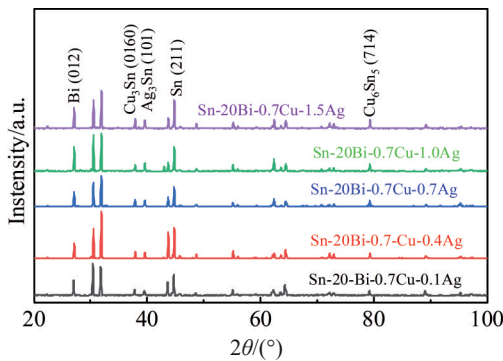


Fig.3 XRD patterns of Sn-20Bi-0.7Cu-xAg alloys

Consequently, during thermal aging, the growth of the Cu₃Sn is more significant compared to that of the Cu₆Sn₅^[18-19]:



However, when the supply of both Cu and Sn atoms is sufficient, the growth of IMCs in the solder joint depends on the activation energy required to form the particular IMC.

Fig.4 shows the optical microscope (OM) images of the Sn-20Bi-0.7Cu-1.0Ag solder after aging at 85 °C for 200 h. Two visible regions of the β-Sn phase and Ag₃Sn eutectic phase of Cu₆Sn₅ can be observed in the microstructure of the solder.

The micro-cracks are generated in the Cu₆Sn₅ layer, and Bi atoms continue to diffuse into the Cu₃Sn layer, which results in the formation of voids. During the growth of IMCs, the

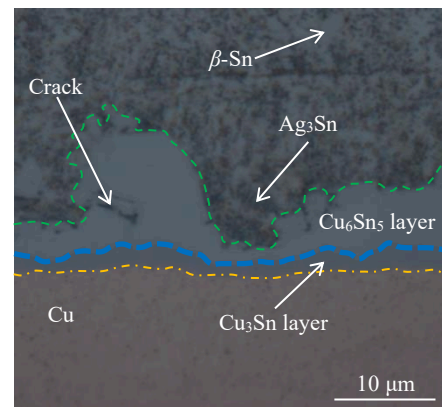


Fig.4 Bulk microstructure of Sn-20Bi-0.7Cu-1.0Ag aged at 85 °C for 200 h

solubility of Bi in Cu₃Sn is lower than that of Cu₆Sn₅, so Bi will precipitate, and Cu₆Sn₅ will be converted into Cu₃Sn. After aging for 200 h, Cu₆Sn₅ and the solder layer form a Bi barrier layer. Besides, the Cu₆Sn₅ particles in the matrix continue to accumulate at the interface; however, the Bi layer hinders the annexation and growth of interface compounds. Therefore, the morphology of the interface layer is still scallop-type and not smooth.

Fig.5 depicts the SEM morphology and EDS results of IMC for Sn-20Bi-0.7Cu-1.0Ag aging solder on Cu substrate. The scallop-type morphology is observed in all solder joints. During soldering, solder paste will melt and wet Cu substrate, resulting in the formation of the IMC layer along the

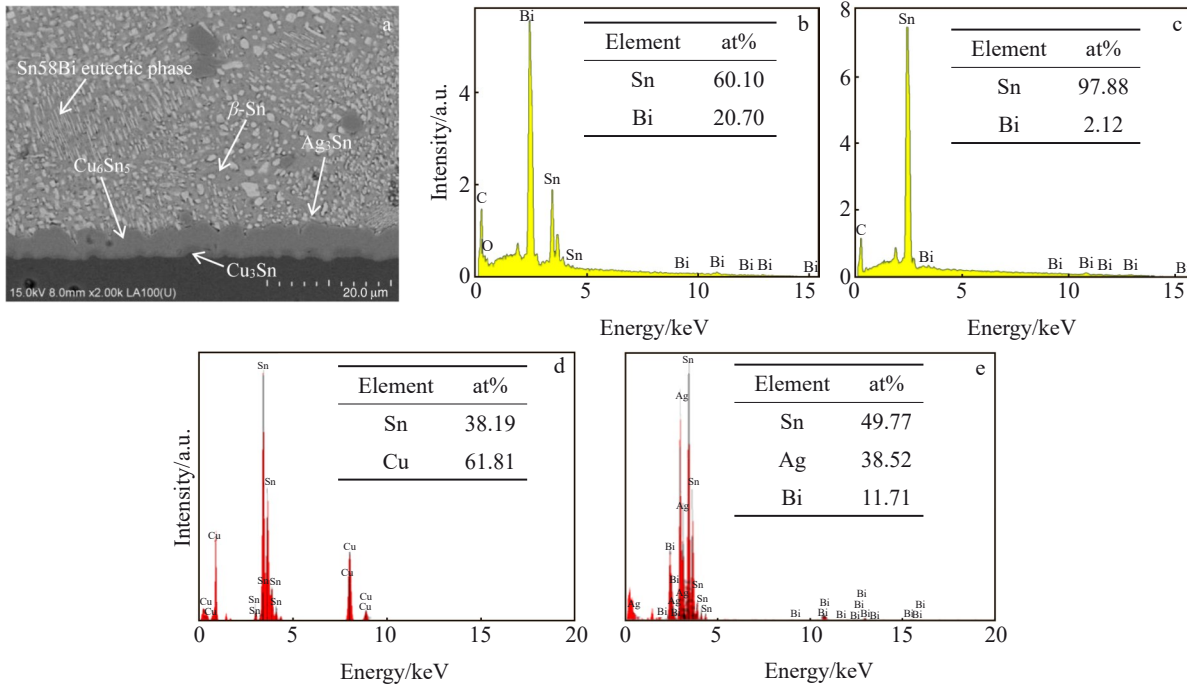


Fig.5 SEM morphologies of Sn-20Bi-0.7Cu-1.0Ag/Cu bulk aged at 85 °C for 200 h (a), and EDS results of Sn-58Bi (b), β -Sn (c), Cu_6Sn_5 (d), and element detected (e)

substrate. The diffusion of Cu atom from the Cu substrate and Sn atom from solder to the interface between melt solder and substrate will continue until Sn becomes supersaturated. The Cu_6Sn_5 IMC is first precipitated from the supersaturated Sn liquid phase.

SEM image and EDS result in Fig.5d show that the IMC phase formed during early soldering is considered to be Cu_6Sn_5 referring to the atomic ratio of Cu:Sn (nearly 6:5). The dendritic Ag_3Sn phase is distributed in the β -Sn matrix. After aging, the segregation of Bi is improved, and the Sn-Bi eutectic phase is mainly distributed around the Cu_6Sn_5 phase. Generally, the microstructure of the Sn-20Bi-0.7Cu-1.0Ag/Cu layer after aging consists of β -Sn phases (light color), dendritic Ag_3Sn phase, Sn-Bi eutectic phase, scallop-type Cu_6Sn_5 phase and lamellar Cu_3Sn phase.

Fig. 6 shows TEM image and SAED patterns of the Sn-20Bi-0.7Cu-1.0Ag/Cu, and we reconfirm the existence of the

primary phase. Also, Ag_3Sn particles are found in the matrix, suggesting that the addition of Ag not only strengthens the third phase but also refines the particles.

Fig. 7 shows the HRTEM micrograph of Fig.6a. The angle between the crystal planes of β -Sn crystal grains and Ag_3Sn particles is 110.5°, and the measured crystal plane spacing is the spacing between $\{012\}$ crystal plane family and $\{001\}$ crystal plane family. It can be seen that when the solder alloy is solidified, the β -Sn crystal grains firstly nucleate on the (020) crystal plane and grow on the (200) crystal plane of the Ag_3Sn particles.

3 Discussion

Based on Ref. [18], one of the famous approaches is to calculate the activation energy of the Cu_6Sn_5 and Cu_3Sn IMCs derived from the data acquired from the thermal aging test. The growth of total IMC layers under both thermal conditions

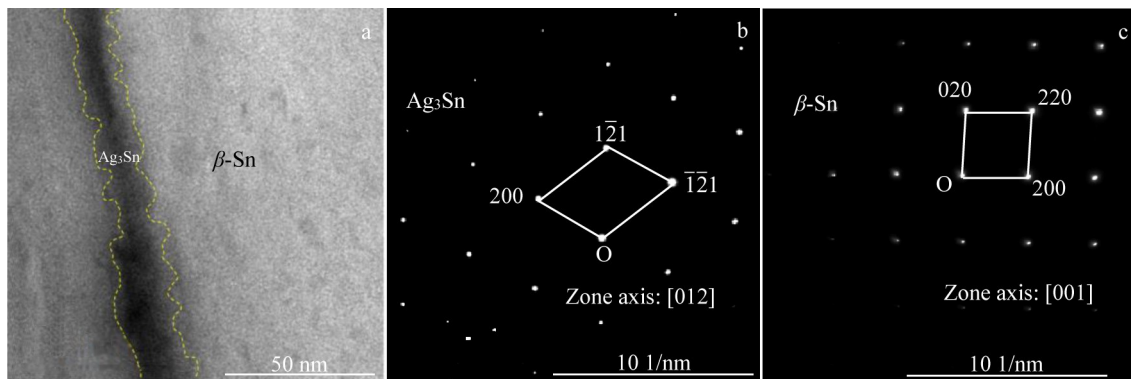


Fig.6 TEM micrograph of Sn-20Bi-0.7Cu-1.0Ag (a) and SAED patterns of Ag_3Sn (b) and β -Sn (c) acquired from the aperture area in Fig.6a

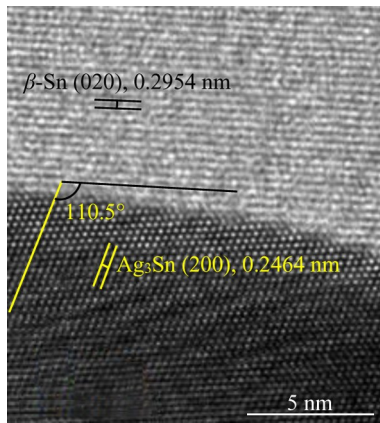


Fig.7 Micro area district of Fig.6a by HRTEM

can be explained by the following equation^[20]:

$$x - x_0 = At_{\text{eff}}^n \quad (4)$$

where x is the total thickness of both IMC layers at time t_{eff} , x_0 is the as-soldered total thickness of the IMC layer, A is the growth constant, and n is the time exponent.

The growth of interfacial IMCs can be divided into three stages^[21–22]. The first stage is the reaction-diffusion stage, with a maximum growth rate and n value tending to 1. The second stage is the grain boundary diffusion stage, and the growth rate begins to decrease, with n value between 0.5 and 1. The third stage is the body diffusion stage, with the slowest growth rate and n value less than 0.5.

According to the slope, n value can be obtained. The growth stage of IMC can be determined. After aging for 10 h, all of the n values are less than 0.5. It can be seen from Table 1 that the growth of the Cu_6Sn_5 layer enters into the third stage after aging for more than 10 h, which is the bulk diffusion stage with the slowest growth rate. In addition, when the welding enters into the third stage, the growth of the Cu_6Sn_5 layer is in the second stage with grain boundary diffusion. The first stage is the reaction-diffusion stage, where the growth rate is the largest, and the value of n approaches 1, which is the welding process. Since the Cu_3Sn layer is located between Cu and Cu_6Sn_5 , two growth mechanisms are possible. At the Cu/ Cu_3Sn interface, the layer grows due to the reaction between Cu and diffused Sn according to Eq. (1). At the Cu_6Sn_5 / Cu_3Sn interface, the layer grows due to interaction between Cu_6Sn_5 and diffused Cu.

The relative ratio of Cu and Sn diffusivities in Cu_3Sn determines whether Eq. (2) or Eq. (3) dominates. Usually, the Cu diffusivity in Cu_3Sn is about ten times less than Sn

Table 1 Time exponent (n) as a function of aging time

Soder	$n_{\text{Cu}_6\text{Sn}_5}(10\text{ h})$	$n_{\text{Cu}_6\text{Sn}_5}(500\text{ h})$	$n_{\text{Cu}_3\text{Sn}}(500\text{ h})$
Sn-20Bi-0.7Cu-0.1Ag	0.46	0.32	0.047
Sn-20Bi-0.7Cu-0.4Ag	0.45	0.31	0.041
Sn-20Bi-0.7Cu-0.7Ag	0.45	0.32	0.039
Sn-20Bi-0.7Cu-1.0Ag	0.42	0.32	0.041
Sn-20Bi-0.7Cu-1.5Ag	0.49	0.33	0.044

diffusivity at 85 °C. This suggests that Cu_3Sn layer formation is given by Sn diffusion, and the layer grows at the Cu/ Cu_3Sn interface. Based on the previous discussion, it can be reasonably suggested that the Cu_3Sn layer formation is limited by Sn diffusion. Generally, element diffusion through grain boundaries is faster than through the grain interior. It has been shown that 1wt% of Bi may lead to an approximately 10% decrease in the rate constant^[23].

The reduction of the intermetallic growth rate decreases the rate of joint degradation and increases the durability. The observed obedience to the parabolic law indicates that the Cu_6Sn_5 layer formation is diffusion-limited (Fig. 8). The diffusion coefficients of Sn and Cu in Cu_6Sn_5 at 85 °C are comparable. This observation suggests that the Cu_6Sn_5 layer probably grows by counter-diffusion of Sn and Cu. Table 1 compares the parabolic rate constants from the present study with the rate constants for the Cu_6Sn_5 growth studied previously. The activation energies are comparable, with only a slightly higher value for Cu_6Sn_5 . The interface layer consists of two parallel layers of Cu_3Sn and Cu_6Sn_5 . Cu_6Sn_5 is formed during soldering and grows parabolically during subsequent solid-state aging. Cu_3Sn is formed during solid-state aging, and the growth rate is decreased by Bi and Ag in the lead-free solder. It is suggested that Cu_3Sn grows by Sn diffusion. Since indium and possibly also Bi can substitute Sn in intermetallic compounds, Cu_3Sn or Ag_3Sn compounds may form at Cu_3Sn grain boundaries where they inhibit Sn diffusion.

The parabolic rate constant of the intermetallic layer formation is increased, and some Sn is substituted by Bi and Ag_3Sn in Cu_6Sn_5 at the Sn-20Bi-0.7Cu-1.0Ag/Cu solder joint interfaces. It is suggested that Bi can increase copper diffusion in Cu_6Sn_5 and lead to the formation of Ag-based compounds at high concentrations. At later stages of aging, the Cu_6Sn_5 layer

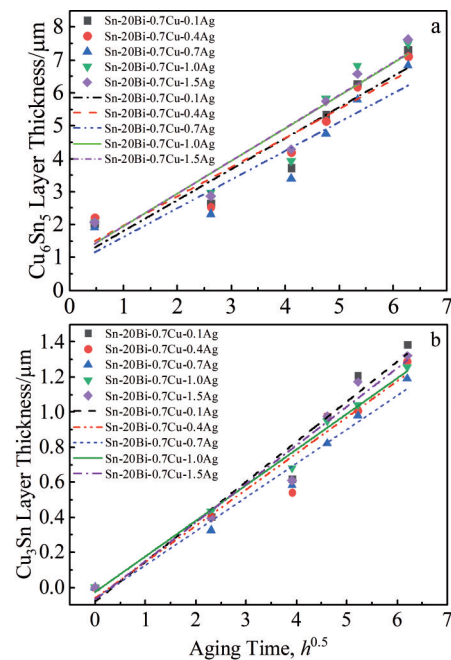


Fig.8 Average thickness of IMCs Cu_6Sn_5 (a) and Cu_3Sn (b) at 85 °C

growth is further enhanced by intermetallic phase precipitation in the solder bulk, which may lead to premature degradation of the solder joint. The Bi and Ag concentration should be lowered to avoid the excessive precipitation of Cu_6Sn_5 in bulk.

4 Conclusions

1) With increasing Ag content in the Sn-20Bi-0.7Cu-xAg solders, the growth of the Cu_6Sn_5 layer is suppressed and expected to be prevented in the horizontal direction until the grains start to impinge each other. The scallop-type shape of this phase is probably a result of the grain coarsening, and it disappears at later stages of aging, suggesting a change in the growth mechanism to the steady growth in the direction perpendicular to the interface. When the solder alloy is solidified, the β -Sn crystal grains firstly nucleate on the (020) crystal plane and grow on the (200) crystal plane of the Ag_3Sn particles.

2) The growth index n of Cu_6Sn_5 and Cu_3Sn is calculated, and the growth process of the Cu_6Sn_5 layer can be separated. Bi, Cu_6Sn_5 , and Ag_3Sn inhibit the growth of Cu_3Sn . The growth index is very low for Cu_6Sn_5 . And 0.7wt% Ag has the best effect on the stability of Sn-20Bi-0.7Cu solder.

References

- 1 Abteu M, Selvaduray G. *Materials Science and Engineering R: Reports*[J], 2000, 27(5-6): 95
- 2 Zajączkowski A. *Calphad*[J], 2018, 60: 50
- 3 Silva B L, Garcia A, Spinelli J E. *Journal of Alloys & Compounds*[J], 2017, 691: 600
- 4 Chen C M, Huang C C. *Journal of Alloys & Compounds*[J], 2008, 461(1-2): 235
- 5 Chou C K, Hsu Y C, Chen C. *Journal of Electronic Materials*[J], 2006, 35(8): 1655
- 6 Miao H W, Duh J G, Chiou B S. *Journal of Materials Science Materials in Electronics*[J], 2000, 11(8): 609
- 7 Miao H W, Duh J G. *Materials Chemistry & Physics*[J], 2001, 71(3): 255
- 8 Mokhtari O, Zhou S, Chan Y C et al. *Materials Transactions*[J], 2016, 57(8): 1272
- 9 Butrymowicz D B, Manning J R, Read M E. *Journal of Physical & Chemical Reference Data*[J], 1977, 6(1): 1
- 10 Krishnamurthy R, Srolovitz D J, Mendelev M I et al. *Acta Materialia*[J], 2007, 55(15): 5289
- 11 Oikawa H, Hosoi A. *Scripta Metallurgica*[J], 1975, 9(8): 823
- 12 Hopkins S C, Tan K S, Pong I et al. *Defect & Diffusion Forum*[J], 2006, 258-260: 152
- 13 Chou T H, Huang J C, Yang C H et al. *Acta Materialia*[J], 2020, 195: 71
- 14 Mei Z, Sunwoo A J, Morris J W. *Metallurgical Transactions A*[J], 1992, 23(3): 857
- 15 Zhang X, Matsuura H, Tsukihashi F et al. *Materials Transactions*[J], 2012, 53(5): 926
- 16 Mul D, Huangl H, McDonald S D et al. *Materials Science & Engineering A*[J], 2013, 566: 126
- 17 Hu R Z, Zeng M Q, Zhu M. *Electrochimica Acta*[J], 2009, 54(10): 2843
- 18 Lin F, Bi W, Ju G et al. *Journal of Alloys & Compounds*[J], 2011, 509(23): 6666
- 19 Cai H G, Liu Y, Zhang H et al. *Rare Metal Materials and Engineering*[J], 2020, 49(1): 27
- 20 Dybkov V I, Meshkov E S. *Soviet Powder Metallurgy and Metal Ceramics*[J], 1992, 31(11): 970
- 21 Meinshausen L, Frémont H, Weide-Zaage K et al. *Microelectronics Reliability*[J], 2015, 55(1): 192
- 22 Yang L T, Huang Y K, Yang H H et al. *Solar Energy Materials & Solar Cells*[J], 2014, 123: 139
- 23 Rizvi M J, Chan Y C, Bailey C et al. *Journal of Alloys & Compounds*[J], 2006, 407(1-2): 208

Ag含量对Sn-20Bi-0.7Cu焊料中金属间化合物形成与生长的影响

陈东东¹, 秦俊虎², 甘有为¹, 张欣², 白海龙³, 赵玲彦³, 易健宏¹, 严继康^{1,4}

(1. 昆明理工大学 材料科学与工程学院, 云南 昆明 650093)

(2. 云南锡业锡材有限公司, 云南 昆明 650217)

(3. 云南锡业集团(控股)有限责任公司 研发中心, 云南 昆明 650000)

(4. 西南石油大学 工程学院, 四川 南充 637001)

摘要: 研究了Sn-20Bi-0.7Cu-xAg焊料凝固和时效过程中的物相生长动力学。通过实验和数值分析相结合分析了Ag含量和时效条件对界面结构和生长的影响, 实验中对Sn-20Bi-0.7Cu分别添加了质量分数0.1%、0.4%、0.7%、1.0%、1.5%的Ag。为验证焊接接头的服役可靠性, 在85℃和85%的湿度条件下, 将接头放置0、10、30、50、100、200和500h。采用扫描电镜等设备分析时效过程中界面化合物的形貌、厚度和分布, 分析了 β -Sn的形核界面和取向。结果表明, 焊料中Ag含量的增加可以抑制界面 Cu_6Sn_5 层的生长, 等温时效期间金属间化合物($\text{Cu}_6\text{Sn}_5+\text{Cu}_3\text{Sn}$)的生长为扩散控制机制。焊接时形成的扇贝状表面在时效时消失, 这表明在垂直于界面方向上的生长机制变为稳定性增长, 说明 Ag_3Sn 有效降低了 Cu_6Sn_5 的生长动力。

关键词: Sn-20Bi-0.7Cu; 金属间化合物; 凝固; 界面结构; 生长动力学